Responsive Janus and Cerberus Emulsions via Temperature-Induced Phase Separation in Aqueous Polymer Mixtures

Marko Pavlovic,[a] Markus Antonietti,[a] Bernhard V. K. J. Schmidt,[b]* and Lukas Zeininger[a]*

[a] Department of Colloid Chemistry, Max-Planck Institute of Colloids and Interfaces, Am Mühlenberg 1, 14476 Potsdam, Germany (e-mail: lukas.zeininger@mpikg.mpg.de)

[b] School of Chemistry, University of Glasgow, G128QQ Glasgow, United Kingdom (e-mail: bernhard.schmidt@glasgow.ac.uk)

Abstract

Complex aqueous emulsions represent a promising material platform for the encapsulation of cells, pharmaceuticals, or nutrients, for the fabrication of structured particles, as well as for mimicking the barrier-free compartmentalization of biomolecules found in living cells. Herein, we report a novel, simple, and scalable method of creating multicomponent aqueous droplets with highly uniform internal droplet morphologies that can be controllably altered after emulsification by making use of a thermal phase separation approach. Specifically, temperature-induced phase separation inside as-formed emulsion droplets comprising aqueous mixtures of two or more hydrophilic polymers allows for the generation of Janus and Cerberus emulsion droplets with adjustable internal morphologies that are solely controlled by a balance of interfacial tensions. We demonstrate our approach by applying both, microfluidic and scalable batch production, and present a detailed model study with predictive capabilities that enables fine-tuning and dynamically altering the droplet morphology as a function of types, molecular weights, and hydrophilicities of the polymers as well as the surfactant hydrophilic-lipophilic balance. The ability to rationally design complex aqueous emulsion droplets with previously unattainable dynamic control over their morphologies after emulsification entails the potential to design new responsive soft materials with implications for a variety of applications beyond encapsulation, including the design of complex adaptive and self-regulating materials, e.g. for chemical and biological sensing applications.

1. Introduction

Water-water phase separation in mixtures of salts and polymers via associative or segregative mechanisms is a well-known tool for the generation of aqueous multiphase systems or coacervates, respectively.[1,2] The ability to create multiple biocompatible phases with water as a common solvent provides a powerful tool for a diverse set of applications, including density-based separation and fractionation of particles or cells,[3] encapsulation, enrichment and delivery of active components,[4] drop-based sequencing or compartmentalization of biologicals or nutrients,[5] as well as for mimicking the crowded microenvironment found in living cells.[6,7]

One of the most popular examples of phase-separated aqueous polymer mixtures is based on the hydrophilic polymer pair poly(ethylene glycol) (PEG) and dextran (Dex) that, when exceeding a critical polymer concentration (commonly referred to as the binodal), turn biphasic and form an aqueous two-phase system (ATPS). Although phase-separated, the interfacial tension between the phases of such ATPS is ultralow (~1-100 µN m^{-1}), thus generating a semipermeable phase boundary enabling mass transfer of small water-soluble molecules across the interface.[8,9] Larger active components including catalysts or reactants can be enriched in the interior based on preferential solubility or physically trapped at the interface.[10,11] Therefore, the water-water system can be used to sequester molecular or macromolecular components, such as functional biomolecules, DNA, or to support enzymatic activity, but also to gain spatial and temporal control of reactions and pathways, all together laying the basis for the development of artificial bioreactors and protocells.[12-14]

In this context, the development of multi-compartment, i.e. complex emulsion droplets has received considerable attention over the past decades.[15-17] Depending on the fabrication technique, a variety of droplet geometries are accessible, including multiple emulsions (i.e. emulsions-of-emulsions),[18] encapsulated core-shell structures (including onion-shaped droplets),[19] as well as anisotropic emulsion droplets with linear morphologies.[20,21] The latter include two-phase systems commonly referred to as Janus emulsions (droplets with two faces

of differing chemistries that can be individually addressed),[22] and layered three-component "Cerberus" emulsion droplets, named after the three-headed dog of Roman mythology.[23] Such structured liquid droplets are intriguing building blocks for a variety of applications, including for the fabrication of anisotropic particles,[24,25] the encapsulation and release of components,[26] to modulate optical properties of materials,[27-29] and as transducers in liquid sensing applications.[30,31] However, despite the omnipresence of single phase aqueous emulsion technologies in a large number of products, thus far the vast majority of reported examples of layered complex emulsion droplets are based on organic fluids, including hydrocarbons, fluorocarbons, mineral and vegetable oils, or liquid crystals,[32-35] and comparatively few techniques are available for the generation of complex, all aqueous emulsion droplets. This shortage particularly extends to responsive aqueous multicomponent droplets with uniform morphologies that can be controllably altered after emulsification.

The difficulty of stabilizing and influencing aqueous multiphase systems inside emulsion droplets stems from their intrinsic physicochemical properties, such as their characteristically low interfacial tension, the related broad interfacial width, as well as the nature of the formation techniques.[36] For instance, while microfluidic technologies have been shown to impart exceptional practicability for producing a large variety of complex emulsions with controllable sizes, shapes, and compartments, their applicability for the production of purely aqueous-based multiphase droplets has been limited due to the ultralow interfacial tensions and the associated difficulty to stabilize individual droplet phases.[37] Alternative current approaches for the production of complex aqueous emulsions are based on a triggered coalescence of droplets by overcoming of the droplet stabilization potential, e.g. by shear-mixing of phase separated aqueous polymer mixtures,[38] or rely on externally triggering a polymer phase-separation inside as-formed emulsion droplets. To this end, an induced mass transfer from the dispersed phase, e.g. via creating an osmotic stress imbalance[39,40] or temperature-induced water extraction[41,42] has been shown to change the local polymer concentration and can thus induce phase-separation for the formation of complex aqueous emulsions. However, these approaches result in only statistical control over the final droplet

geometry and require a precise control over the degree of water extraction that is necessary to prevent rupture of the droplet network. As a result, current methods for the production of complex aqueous emulsion droplets are usually associated with one or more of the following drawbacks: the need for sophisticated and expensive equipment, complicated manufacturing, multiple fabrication steps, and/or a low degree of control over the final droplet structure. In addition, reported examples have yet to create a system that allows to controllably vary the droplet geometry ultimately leading to micro-colloidal systems that can specifically present and hide liquid-liquid interfaces, with the potential to react to environmental or (bio-)chemical cues.

Herein, we introduce a novel, simplified technique for the one-step fabrication of complex aqueous emulsions with highly controlled and reconfigurable internal morphologies based on a thermal phase separation approach. Specifically, we produced aqueous Janus and Cerberus emulsion droplets by making use of the temperature sensitivity of phase separation in aqueous polymer mixtures. We selected aqueous mixtures of two or more polymers that exist as a single phase at the preparation temperature but return to their thermodynamically preferred phase-separated state at room temperature (RT). At the preparation temperature, single-phase aqueous polymer mixtures were easily emulsified using batch-scale or microfluidic techniques. Upon returning to room temperature (RT), polymer phase-separation inside as-formed emulsion droplets was induced to yield structured complex emulsion droplets with highly uniform composition (Figure 1). Once formed, the phase-separation inside droplets could be reversibly switched between mixed and phase-separated as controlled by the temperature. In addition, as a result of the morphology of as-formed complex droplets being exclusively controlled by a balance of interfacial tensions, our approach enabled fine-tuning of the internal droplet morphologies as a function of type, ratio, hydrophilicity, and molar mass of the employed polymers, as well as type and hydrophilic-lipophilic balance (HLB) of the employed surfactants. The same principles of droplet transformation were extended to a four-phase system, thereby generating reconfigurable Cerberus emulsion droplets of higher-order complexity. In addition, we demonstrated the potential use of our aqueous complex emulsions for the fabrication of responsive materials. The latter is showcased by a dynamic and reversible

reconfiguration of droplet morphology induced by (bio-)chemical triggers, i.e. a variation of surfactant composition or an enzymatic reaction-driven reorganization of the internal droplet morphology thus leading to a system capable of optical visualization of enzymatic activity.

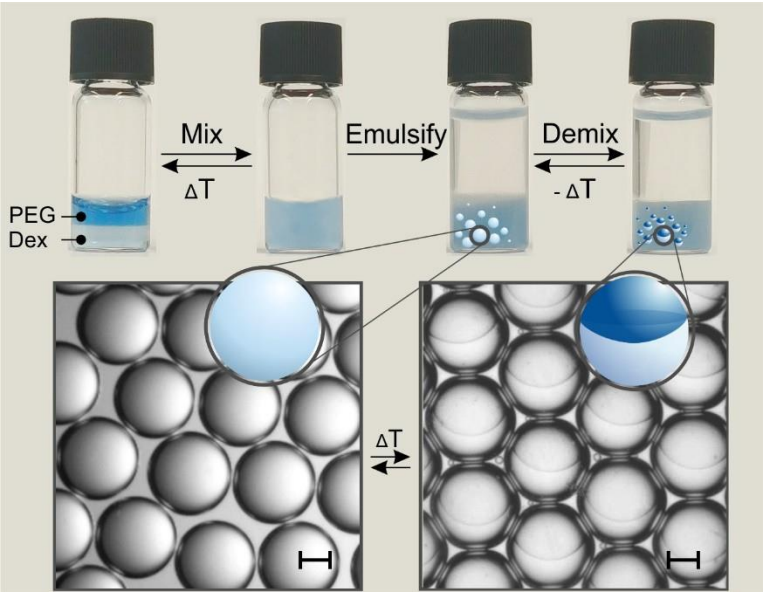

Figure 1. Temperature-controlled phase-separation of aqueous polymer mixtures can be used to create complex aqueous emulsions. At certain concentrations, aqueous solutions of hydrophilic polymers (displayed is an aqueous solution of PEG (35 kDa) and Dex (40 kDa)) are miscible at low temperatures and can be emulsified to yield single phase emulsion droplets. Upon returning to RT, polymer phase separation inside as-formed emulsion droplets leads to the formation of Janus emulsions with highly controllable and uniform internal droplet morphologies. The dye reactive blue 160 selectively partitions into the PEG phase. Scale bar: 50 µm.

2. Materials and methods

2.1. Chemicals. All listed chemicals were of analytical grade and used as received without any further purification: Hydrophilic polymers: poly(ethylene glycol) (PEG) 3.35k (Sigma-Aldrich), PEG 35k (Sigma-Aldrich), Ficoll 400 (Sigma-Aldrich), Polyvinylpyrrolidone 58 k (Acros Organics); Dextran 40k (TCI Europe), Pullulan (TCI Europe); Dextran 500k (Alfa Aesar); Surfactants: Span 20 (Sigma-Aldrich), Span 80 (Sigma-Aldrich), and Span 85 (Sigma-Aldrich); Enzyme: Dextranase from *Penicillium sp.* (Sigma-Aldrich); Dye: Reactive blue 160 (Sigma-Aldrich); Continuous phase: Tetradecane (Sigma-Aldrich). Deionized (DI) water was used in all experiments.

2.2. Instruments. UV-Vis absorption spectra were recorded using a T70+ UV/Vis spectrophotometer from PG Instruments Ltd. Isothermal titration calorimetry (ITC) measurements were performed with a VP-ITC calorimeter (Northampton, MA). Microscope images were recorded on a Bresser Trino and a Bresser Science IVM-401 inverted microscope. For recording top and bottom-view micrographs, emulsion droplets were deposited into an Invitrogen Attofluor Cell Chamber from Thermo-Fisher Scientific. Side-views of the droplets were taken using a horizontal microscopy setup on a Krüss contact angle measuring system G10. The droplets were placed upright in a 0.2 mm cuvette. A white screen illuminated the sample from the back. For the preparation of monodispersed complex aqueous emulsion droplets we used a commercial microfluidic setup. The flow rates were controlled by a Fluigent Flow-EZ pressure control platform and we used a flow focusing hydrophilic glass large droplet junction chip with a 100 µm channel depth, purchased from Dolomite Microfluidics.

2.3. Determination of ATPS Phase Diagrams. The phase diagrams of aqueous polymer mixtures were routinely determined by turbidimetric and cloud point titration for each polymer combination in H_2O as described by Albertsson.[1] In brief, for the phase diagram determination using the turbidimetric titration method we first prepared concentrated stock solutions (20 wt.%) of two different hydrophilic polymers in DI water and the solution of component 2 was added stepwise to a stirred solution of component 1. At the cloud point, the mixture turned turbid indicating the formation of a two-phase mixture. Knowing the concentrations of the stock solutions, the polymer composition at the cloud point could be readily calculated. Subsequently, the mixture was diluted with small volumes of DI water until the cloud point was crossed. The solution was repeatedly taken above and below the cloud point by subsequent addition of the stock solution of component 2 or DI water (zig-zag line in Figure S1). This procedure was repeated until the full binary was recorded. In addition, we recorded the phase diagrams using the

cloud point titration method. Here, we started by preparing 4 g of a concentrated stock solution of the two polymers of known composition in DI water within the 2-phase region of the phase diagram. Mixtures of known compositions were then diluted down using DI water, until, at the cloud point, they turned clear indicating the formation of a single phase. The resultant polymer composition at the point of transition was calculated. In both methods the data sets were collected at three different temperatures, namely 5°C, RT (25°C), and 50°C, to reveal the temperature dependency of the phase transition in polymer mixtures. To verify these results and to precisely quantify the temperature dependency of the phase transition in two-polymer mixtures, we recorded isothermal titration calorimetry (ITC) dilution profiles. In ITC experiments, concentrated stock solutions of an aqueous polymer mixture (total polymer concentration: 10 wt.%; total volume: 0.73 mL) of known composition were diluted down with equal volumes of DI water (dilution speed: 10µL min^{-1}) until the binary was crossed (see Figure S1). In the dissolution heat profiles a maximum in the recorded dilution heat indicated the point of transition to a single-phase aqueous polymer mixture. The resultant polymer composition at the point of transition was back-calculated, knowing the total volume of added DI water, to precisely quantify the polymer concentrations at the binodal line. For the tested polymer combinations, we observed that the binodal at lower temperature was above the binodal at room temperature. To display the temperature dependency of phase transition, we recorded temperature-dependent UV-Vis absorption measurements (Figure S2) of four aqueous polymer mixtures of known compositions.

2.4. General procedure for the fabrication of aqueous Janus emulsion droplets. In a typical experiment we started by preparing a concentrated stock solution of two hydrophilic polymers in DI water in the desired volume ratio in the phase separated state. Similarly, to the turbidimetric determination of the phase diagrams described above, this mixture was subsequently diluted down by stepwise addition of DI water. At concentrations close to the binodal, the phase separation of ATPS was significantly slowed down indicating overall polymer concentrations in the 2-phase regime, but close to the binodal line. In cases where the cloud point was crossed, the mixtures turned clear indicating the formation of a one-phase system. In these cases, a small volume of concentrated polymer stock solution was added in order to return to the phase-separated state right above the binary at room temperatures. These phase-separated mixtures were subsequently cooled down to ~7°C in a water bath resulting in phase mixing. Once cooled and miscible, the two polymer mixtures were emulsified within a surfactant (1 wt.% Span 80 or Span 85) containing hydrocarbon oil (tetradecane) at 7°C, either in bulk by shaking (vortex-

mixing) or by using a flow focusing glass hydrophobic microfluidic chip with a 100 µm channel depth (Dolomite Microfluidics). The temperature of 7°C was chosen to ensure the tetradecane was kept above its freezing temperature. In the vortex-mixing approach, 100 µL of the cooled aqueous polymer solution was injected into 1000 µL of the cooled surfactant solution in tetradecane. Once formed, the emulsions were allowed to warm up to RT to induce phase separation within the droplets. In the microfluidic production route, cooled solutions of both the surfactant containing hydrocarbon oil and the aqueous polymer mixture were injected into the microfluidic chips. The flow rates were controlled by a Fluigent pressure MFCS-EZ pressure controller, thus providing the ability to vary the size of the droplets (from ~50 µm to 150 µm). The resulting emulsion droplets phase-separated within minutes when kept at RT and were stable during the time periods used (in the order of days). A cooling of the emulsion droplets below RT resulted in phase mixing, which occurred in the timescale of hours.

2.5. Fabrication of three phase aqueous 'Cerberus' emulsion droplets. Analogous to the fabrication of aqueous Janus emulsions using a two-phase polymer mixture, for the preparation of three-phase 'Cerberus' emulsion droplets, we started by preparing a concentrated stock solution of three hydrophilic polymers, which was then diluted down using DI water to approach the coexistence line at RT. The starting concentrations of the three polymers were chosen according to the phase diagrams of three phase polymer mixtures. To record the phase diagrams of three phase polymer mixtures we started by preparing stock solutions (20 wt.%) of all three polymers. By varying the polymer concentration of polymers 1 and 2, but keeping a fixed polymer concentration of polymer 3 we obtained phase diagrams of three-phase polymer mixtures as displayed in Figure S11. These phase diagrams of the three-component polymer mixtures feature four regions, a single phase region where polymers 1, 2 and 3 mix, a phase separated three-phase regime, and two 2-phase regimes in which either polymer 1 and 3 or 2 and 3 mix but are phase separated from the polymer rich phase comprising polymer 2 or 1, respectively. For the fabrication of Cerberus emulsion droplets, we used three phase aqueous polymer mixtures that form three separated phases at RT, but transition to a single mixed state at lower temperatures (7 °C).

3. Results and discussion

For the preparation of complex water emulsions based on temperature-induced phase separation in aqueous polymer mixtures, an investigation of the phase diagrams is key (Figure 2a). At low polymer concentrations (i), such aqueous mixtures of two hydrophilic polymers exist as a single phase, and at high concentrations phase separation occurs (iv). The two regions of the diagram are separated by a coexistence curve, commonly referred to as the binodal. In designing our method, we made use of the fact that the location of this binodal curve can be altered by changing the temperature of the system. We recorded the phase diagrams for aqueous two-component mixtures of the hydrophilic polymers at three different temperatures by turbidimetric titration and the cloud point method, as reported previously.[1] We found that for all tested polymer combinations the binodal at 5 °C shifted to higher polymer concentrations. In other words, polymer concentrations that lie in between two binodals (ii and iii) exist as a single phase at lowered temperatures, but return to a two phase mixture when increasing the temperature. It should be noted that in principle, this temperature-induced shift of the binodal can happen vice-versa, as previously observed for ATPS.[1,13] In order to precisely quantify the cloud point of two-polymer mixtures at different temperatures, we recorded isothermal titration calorimetry (ITC) dilution profiles. By diluting down a concentrated stock solution of an aqueous polymer mixture in the two-phase regime with equal volumes of water the binary was crossed. At polymer concentrations close to the coexistence line, we observed a maximum in the dissolution heat, which enabled a quantitative determination and comparison of the cloud point at different temperatures (Figure 2c). For instance, the cloud point of a 1:1 mass ratio of PEG (3.35 kDa) and Dex (40 kDa) decreased gradually from 8.4 wt.% to 7.9 wt.% and 7.4 wt.% overall polymer concentration, for the temperatures of 5, 25, and 50 °C, respectively (Figure 2c). Aqueous mixtures of the polymers in between the two binodals exist as a single phase at lower temperature but return to a two phase mixture at room temperature.

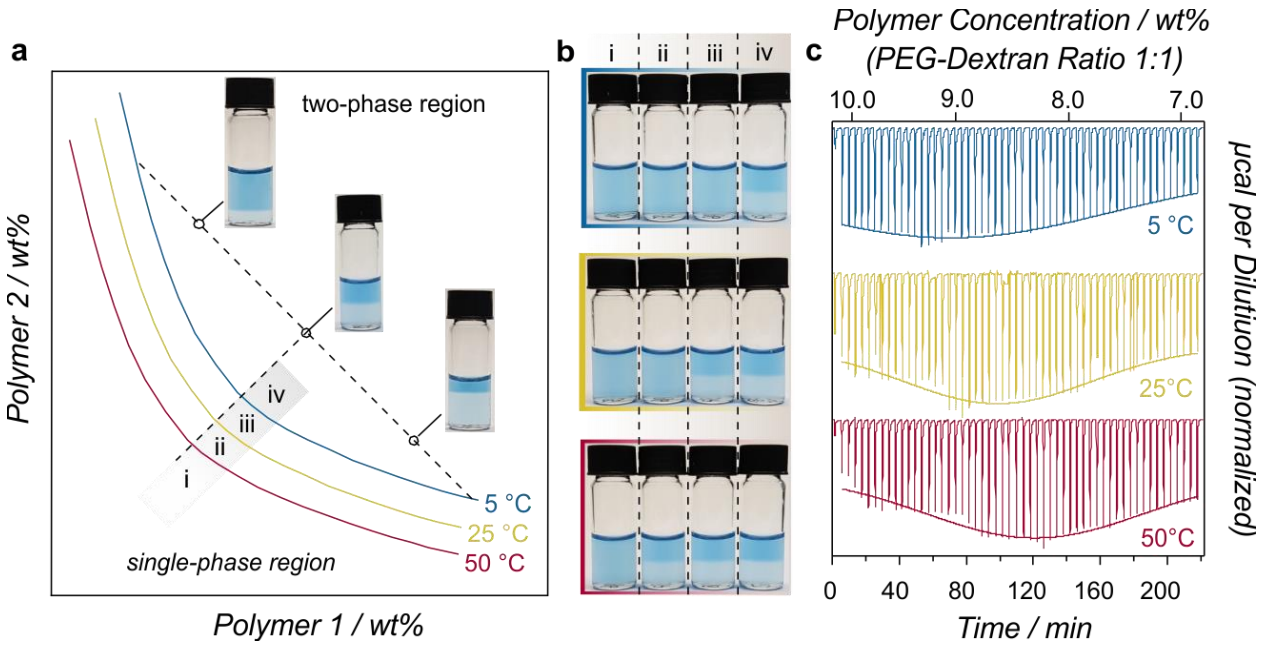

Figure 2. Temperature-dependent phase separation in ATPS. a) Schematic phase diagram of an aqueous mixture of two hydrophilic polymers, outlining the temperature-dependency of the location of the binodal curve that divides the region of component concentrations that will form two immiscible aqueous phases from those that will form a single phase. Inset images display the variation in volume ratio of the constituent phases at three different locations on the tie line. **b**) Images of aqueous solutions containing PEG and Dex polymers at different concentrations illustrating the temperature-dependency of phase separation. **c**) ITC dilution graphs of a 10 wt.% PEG 35 kDa-Dex 40 kDa (ratio: 1:1) solution at three different temperatures.

In our approach, any polymer composition that lies in between two binodals at different temperatures can in principle be used to prepare complex emulsions. With the phase diagrams of aqueous polymer mixtures at different temperatures at hand, we explored the feasibility of using temperature-induced phase separation for the fabrication of complex aqueous emulsions by emulsifying a cooled mixture (5 °C) of PEG and Dex polymers at concentrations close to the binodal line at RT where it exists as single phase. Complex double emulsions were readily produced by shaking or vortex mixing the cooled single-phase aqueous solution in a surfactant-containing hydrocarbon oil (1 wt.% Span 85 in tetradecane). After emulsification, the as-formed emulsion droplets were allowed to warm up to RT, which induced spontaneous phase separation to yield structured complex aqueous emulsion droplets (Figure 1 and Supporting

Video V1). Notably, although more slowly, this phase separation proved to be reversible and phase mixing could be readily induced by cooling the emulsion droplets. Although the resulting complex droplets were polydisperse, the morphology and composition, i.e. the internal shape as well as the volume ratio of the two phases, were highly uniform across the samples. The same principle of droplet formation via thermal phase separation was applicable to the microfluidic production of emulsion droplets, thus generating monodisperse droplets with highly uniform morphologies. All emulsion samples, prepared by shaking, vortex mixing or microfluidics, were stable and did not exhibit any coalescence over a period of at least one week.

As a result of the ultralow interfacial tension between the aqueous polymer phases the droplets assumed a spherical shape and adopted an internal configuration that reflected the balance of interfacial tensions at the external interfaces, i.e. the two individual droplet phases with the continuous oil phase (Figure 3a).[43] In the case of a mixture comprising PEG and Dex polymers, the as-formed complex emulsions adopted a layered 'Janus' morphology with the two individual phases in gravitational alignment, i.e. the PEG-rich phase at the top and the heavier Dex-rich phase at the bottom. We observed chemical partitioning of components that are preferably dissolved in one of the two polymer-rich aqueous phases resulting in directed compartmentalization of solutes such as fluorescent markers, thereby allowing us to easily distinguish between the two phases.

To quantify and analyze the droplet morphology as a function of the type, concentration, molar mass, and hydrophilicity of different polymers we used the contact angle (θ) at the three-phase junction, as determined by side-view images of the respective droplet configurations. As displayed in Figure 3a, two circles that define the inner and outer interfaces of the droplets were used to determine the contact angle by the law of cosines (for details see SI). We found that the internal droplet morphology, as defined by the contact angle is determined by the intrinsic hydrophilicity of the constituent phases. Consequently, the internal shape could be controllably altered by variations in the molar masses of PEG and Dex polymers (Figure 3b).

While droplets formed from PEG 35 kDa and Dex 500 kDa assumed an almost perfect Janus configuration, when prepared in a Span 85 surfactant solution (θ = 99°), a decrease of the molar mass of PEG to 3.35 kDa led to an internal configuration in which the upper phase almost encapsulated the Dex-rich phase (θ = 154°), indicating a preferential decrease in the interfacial tension of the PEG-rich upper phase with the continuous oil phase ($\gamma_{p1/o}$) as a result of the decreased hydrophilicity. The latter is attributed to a decrease in water content in the upper phase, as reported previously. [1] Similarly, a decrease of the molar mass of Dextran to 40 kDa also resulted in an increase of bottom phase hydrophilicity and thus a decrease of the interfacial tension $\gamma_{p2/o}$. Consequently, the changed balance of interfacial tensions resulted in a lowered contact angle of θ = 70°.

To validate the proposed sole dependency of the internal droplet morphology on solely the hydrophilicity of the constituent phases, we determined the contact angle of complex PEG-Dex aqueous droplets with varying volume ratios. The concentration of each polymer in the top and bottom phase is given by the intersection of the tie-line on which that composition lies with respect to the coexistence curve. At the same tie-line, phase-separated ATPS exist as two phases, but differ in volume as indicated in Figure 2a. Thus, the volume ratio could be adjusted by variations in the concentration ratio of the two polymers. In these experiments different polymer concentrations ratios yielded asymmetric double emulsion droplets with varying volume ratios of the individual compartments, whereas the contact angle remained unaffected (Figure 3c).

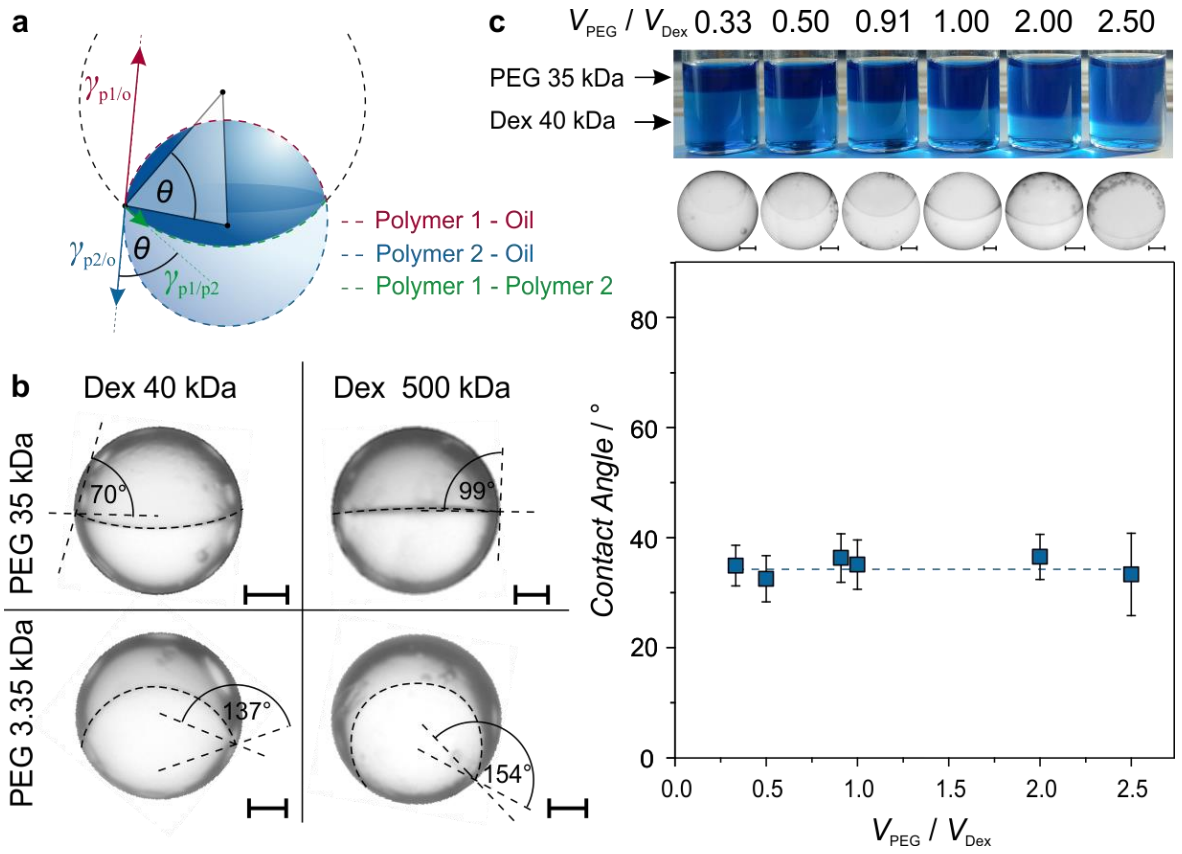

Figure 3. Droplet morphology as a measure of the balance of interfacial tensions. a) Geometry of aqueous Janus droplets: As a result of the ultralow interfacial tensions between the constituent phases the droplets assume a spherical shape and adopt an internal configuration, as defined by the contact angle θ, that reflects the balance of interfacial tensions at the external interfaces. From the two circles that define the inner and outer interfaces of the droplets, the contact angle can be determined using the law of cosines. b**)** Optical micrographs of Janus emulsion droplets formed from PEG and Dex polymers with different molar masses. The droplets assume different internal morphologies due to variations in the hydrophilicity of the resulting compartments. Surfactant: Span 80; Scale bar: 50 µm. **c)** Droplet morphology as a function of the volume ratio of the constituent phases. Surfactant: Span 85. Scale bar: 50 µm. Error of a contact angle determination is given as a standard deviation of contact angles of 10 individual complex droplets.

Beside the molar mass of the constituent polymers, we next anticipated that variations in the polymer composition of the ATPS affect the resulting droplet morphology. Therefore, we produced Janus emulsions from various combinations of suitable pairs of the hydrophilic polymers PEG, Dex, Pullulan, Ficoll, and polyvinylpyrrolidone (PVP). Depending on the

intrinsic hydrophilicity of the polymers, as described by their positioning on the hydrophobic ladder,[1] the resulting Janus droplets assumed morphologies that reflected the balanced interfacial tensions of the polymer phases with the continuous oil phase $\gamma_{p1/o}$ and $\gamma_{p2/o}$. As a result, the morphology of Janus emulsions could be established as a simple indicator to estimate polymer hydrophilicity, which is a key requirement for bioseparation science.[27] For instance, comparing the contact angle of double emulsion droplets formed from PEG and the PEG-compatible hydrophilic polymers PVP, Ficoll, Dex, and Pullulan resulted in an increase of the contact angle θ, which directly correlated to the increased hydrophilicity of the respective polymer rich aqueous phases, as displayed in Figure 4a (similar hydrophilicity as PEG would result in a contact angle of $\theta = 90°$).

This approach for the controlled fabrication of uniform aqueous multiphase droplets could be extended to a more complex system. We leveraged our understanding of the resulting geometries of complex double emulsions to controllably construct three component, i.e. Cerberus emulsion droplets. Similarly to two phase mixtures, we prepared a mixture of three compatible polymers PEG, Dex and Ficoll, at concentrations close to the binodal curve at room temperature and observed a similar temperature-induced phase-separation profile. Subsequent cooling resulted in a single-phase mixture that could be emulsified. As expected, wetting properties of the polymer phases from Janus droplets could be transferred to the Cerberus droplets, as evidenced in side-view images after phases inside the droplet aligned by gravity. As displayed by the side-view micrographs in Figure 4b, the resulting droplets assumed an internal morphology balancing the interfacial tensions at all three external interfaces. The droplet shapes closely followed the observed morphological trend of Janus droplets and confirmed that variations in the hydrophilicity of the constituent phases are an effective parameter to manipulate the balance of interfacial tensions and thus the droplet shape.

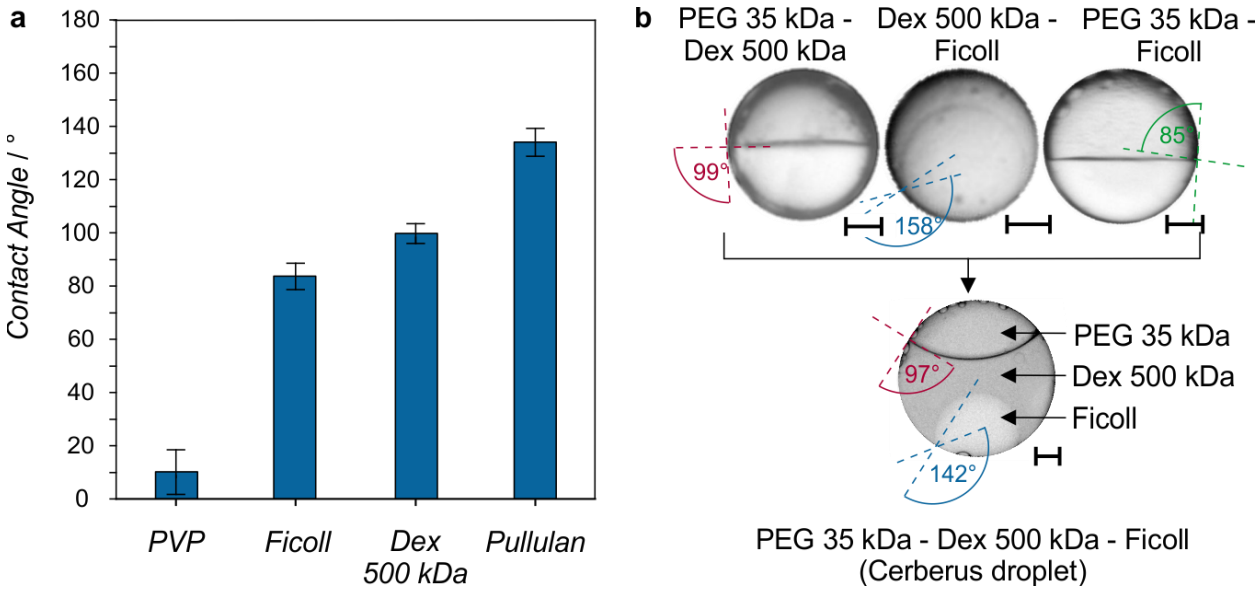

Figure 4. Janus droplet morphology as an indicator of polymer hydrophilicity and to predict the geometry of droplets with higher complexity (Cerberus droplets). a) Graphical representation of the contact angles of Janus emulsions formed from PEG and a series of PEG-compatible hydrophilic polymers. **b)** Optical side-view micrographs of Janus droplets for combinations of the polymers PEG, Dex and Ficoll and internal geometry of a Cerberus emulsion droplets composed of a mixture of all three polymers. Scale bar: 50 µm. Error bars show standard deviation of contact angles of 10 individual droplet samples.

In the following, we anticipated that dynamic variations in the droplet geometry could be used for an *in-situ* monitoring of dynamic variations of interfacial tensions. Leveraging the understanding of a controllable fabrication of complex aqueous emulsion droplets in various shapes we tested whether dynamic morphological transitions could be induced in response to (bio-)chemical cues. A demonstration of the triggerable and reconfigurable nature of the complex aqueous emulsions required to externally influence the balance of interfacial tensions. As such, small variations in surfactant effectiveness, as defined by their hydrophilic-lipophilic balance, transduced into a spontaneous dynamic reconfiguration of the internal droplet morphologies. Whereas droplets prepared in Span 85 (HLB = 1.8) assumed a close to encapsulated morphology ($\theta = 30°$) a stepwise addition of Span 20 (HLB = 8.9) resulted in an 'opening up' of the droplets and a droplet morphology inversion towards a perfect Janus state ($\theta = 87°$). Thus, the internal morphologies could be dynamically and reversibly reconfigured by

inducing small variations in the balance of $\gamma_{p1/o}$ and $\gamma_{p2/o}$, yielding complex emulsions capable of responding to chemical cues.

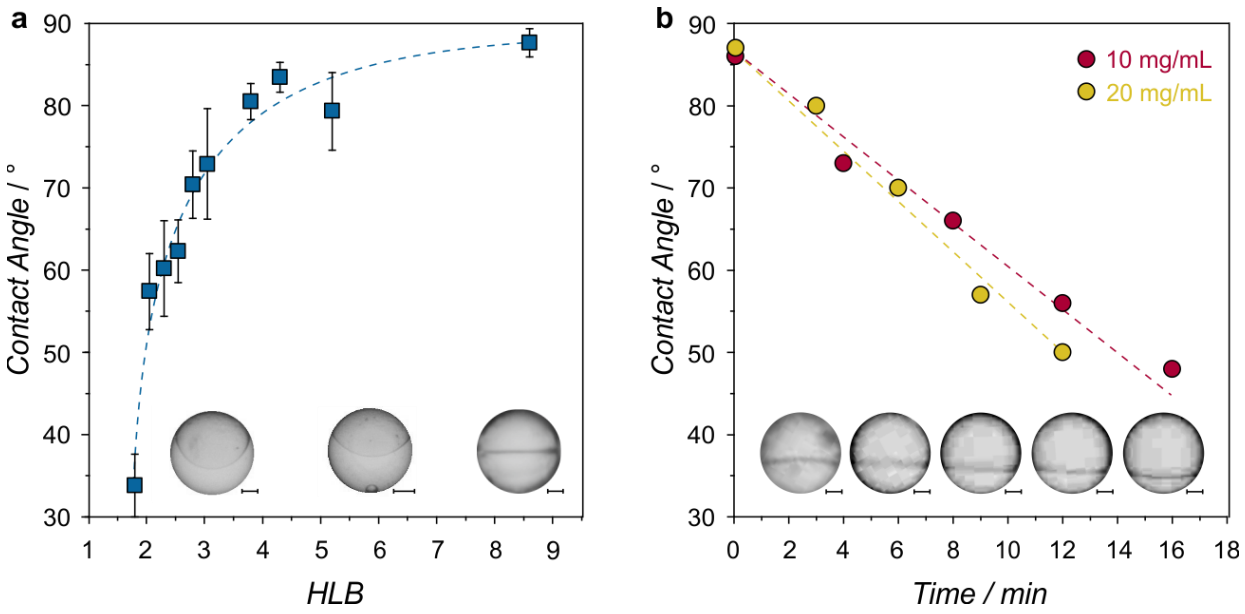

Figure 5. Dynamic morphological reconfiguration of complex aqueous emulsion droplets in response to (bio-)chemical triggers. a) Contact angle of aqueous Janus emulsions as a function of surfactant HLB. **b)** Optical visualization of enzyme activity using dynamically reconfigurable aqueous Janus emulsions: Enzymatic cleavage of high molecular weight dextran inside droplets prepared from PEG and Dex polymers containing dextranase in different concentrations (10 mg/mL or 20 mg/mL) results in variations of the internal droplet geometry as monitored by recording the contact angle at the three-phase contact line. Insets in both graphs show optical side-view micrographs of the aqueous Janus emulsions. Scale bar: 50 µm. Error bars show standard deviation of contact angles of 10 individual droplet samples.

The associated understanding of the chemical-morphological coupling inside aqueous Janus emulsions further enabled us to induce droplet morphological transitions by changing the local interfacial tensions in response to enzymatic activity. We fabricated droplets comprised of a PEG-rich upper phase and dextran-rich bottom phase. These molecularly-crowded compartments of the aqueous double emulsion droplets can be used to encapsulate enzymes, such as dextranase, an enzyme catalyzing the cleavage of 1,6-alpha-D-glucosidic linkages in dextran. An *in-situ* observation of the internal droplet morphology enabled us to optically visualize dextranase activity by means of a reconfiguration of droplet morphology

(Figure 5b). In these experiments we monitored the contact angle of double emulsion droplets prepared from high molecular weight dextran. Upon depolymerization, the droplets reconfigured their morphology, and the contact angle of such emulsions decreased gradually, until mixed. This dependency of the droplet morphological reconfiguration on the dextranase concentration demonstrates that aqueous complex emulsion droplets of controllable composition and dynamically reconfigurable morphology could provide as a novel adaptive material in new and improved emulsion technologies, e.g. for biosensing applications.

4. Conclusions

Taken together, we report a new approach for the facile generation of complex aqueous emulsion droplets with highly uniform and reconfigurable morphologies. Conventional techniques for the fabrication of complex aqueous emulsion droplets rely on droplet coalescence, mass-transfer from the dispersed phase, or the use of sophisticated tapered microfluidic channels, which are limited by their complexity, throughput, or repeatability. By making use of a simple temperature-induced phase separation in aqueous multi-polymer mixtures, the current approach resolves most of these limitations and is easy to scale, i.e. the synthesis of aqueous complex emulsion droplets has been disruptively simplified, which offers exciting possibilities en route towards the fabrication of complex adaptive and self-regulating microreactors. The geometry of our complex aqueous emulsion droplets was found to be mutually controlled by the hydrophilicity and the volume ratios of the two polymer-rich phases. As a consequence, morphological fine-tuning could be achieved by controlled variations in the type or molar mass of constituent polymers as well as the surfactant hydrophilic-lipophilic balance. Dynamic variations of these variables, e.g. in response to (bio-)chemical triggering events demonstrated the adaptive, i.e. reconfigurable and triggerable nature of the aqueous complex emulsion droplets. Multicompartment aqueous emulsion droplets with the characteristic ability to controllably alter their internal morphology and symmetry will provide as new active element for the encapsulation of biologicals, as structural templates to control

the conversion to precision objects, or as broadly deployable transducer in chemo- and bio-sensing platforms.

References

1. Albertsson, P. A. Partition of cell particles and macromolecules. (1960).
2. Chao, Y. & Shum, H. C. Emerging aqueous two-phase systems: from fundamentals of interfaces to biomedical applications. *Chem. Soc. Rev.* **49**, 114-142 (2020).
3. Mace, C. R. *et al.* Aqueous multiphase systems of polymers and surfactants provide self-assembling step-gradients in density. *J. Am. Chem. Soc.* **134**, 9094-9097 (2012).
4. Dupin, A. & Simmel, F. C. Signalling and differentiation in emulsion-based multi-compartmentalized in vitro gene circuits. *Nat. Chem.* **11**, 32-39 (2019).
5. Keating, C. D. Aqueous phase separation as a possible route to compartmentalization of biological molecules. *Acc. Chem. Res.* **45**, 2114-2124 (2012).
6. Booth, R., Qiao, Y., Li, M. & Mann, S. Spatial positioning and chemical coupling in coacervate-in-proteinosome protocells. *Angew. Chem. Int. Edit.* **58**, 9120-9124 (2019).
7. Dewey, D. C., Strulson, C. A., Cacace, D. N., Bevilacqua, P. C. & Keating, C. D. Bioreactor droplets from liposome-stabilized all-aqueous emulsions. *Nat. Commun.* **5**, 4670 (2014).
8. Frampton, J. P., Lai, D., Sriram, H. & Takayama, S. Precisely targeted delivery of cells and biomolecules within microchannels using aqueous two-phase systems. *Biomed. Microdevices* **13**, 1043-1051 (2011).
9. Poudyal, R. R. *et al.* Template-directed RNA polymerization and enhanced ribozyme catalysis inside membraneless compartments formed by coacervates. *Nat. Commun.* **10**, 490 (2019).
10. Albertsson, P.-Å., Cajarville, A., Brooks, D. E. & Tjerneld, F. Partition of proteins in aqueous polymer two-phase systems and the effect of molecular weight of the polymer. *Biochim. Biophys. Acta* **926**, 87-93 (1987).
11. Zhang, J., Hwang, J., Antonietti, M. & Schmidt, B. V. Water-in-water pickering emulsion stabilized by polydopamine particles and cross-linking. *Biomacromolecules* **20**, 204-211 (2018).
12. Koga, S., Williams, D. S., Perriman, A. W. & Mann, S. Peptide–nucleotide microdroplets as a step towards a membrane-free protocell model. *Nat. Chem.* **3**, 720-724 (2011).
13. Long, M. S., Jones, C. D., Helfrich, M. R., Mangeney-Slavin, L. K. & Keating, C. D. Dynamic microcompartmentation in synthetic cells. *PNAS* **102**, 5920-5925 (2005).
14. Dimova, R. & Lipowsky, R. Lipid membranes in contact with aqueous phases of polymer solutions. *Soft Matter* **8**, 6409-6415 (2012).
15. Chu, L. Y., Utada, A. S., Shah, R. K., Kim, J. W. & Weitz, D. A. Controllable monodisperse multiple emulsions. *Angew. Chem. Int. Edit.* **46**, 8970-8974 (2007).
16. Clegg, P. S., Tavacoli, J. W. & Wilde, P. J. One-step production of multiple emulsions: microfluidic, polymer-stabilized and particle-stabilized approaches. *Soft Matter* **12**, 998-1008 (2016).
17. Muschiolik, G. & Dickinson, E. Double Emulsions Relevant to Food Systems: Preparation, Stability, and Applications. *Compr. Rev. Food. Sci. Food Saf.* **16**, 532-555 (2017).
18. Kim, S. H. & Weitz, D. A. One-step emulsification of multiple concentric shells with capillary microfluidic devices. *Angew. Chem.* **123**, 8890-8893 (2011).
19. Haase, M. F. & Brujic, J. Tailoring of High-Order Multiple Emulsions by the Liquid–Liquid Phase Separation of Ternary Mixtures. *Angew. Chem. Int. Edit.* **53**, 11793-11797 (2014).
20. Choi, C. H., Weitz, D. A. & Lee, C. S. One step formation of controllable complex emulsions: from functional particles to simultaneous encapsulation of hydrophilic and hydrophobic agents into desired position. *Adv. Mater.* **25**, 2536-2541 (2013).

21. Zhang, Q. *et al.* Emulsion Agglutination Assay for the Sensing of Zika Virus. *ACS Sensors*, 4, 180-184 (2018).
22. Walther, A. & Müller, A. H. J. C. r. Janus particles: synthesis, self-assembly, physical properties, and applications. *Chem. Rev.* **113**, 5194-5261 (2013).
23. Fryd, M. M. & Mason, T. G. Cerberus nanoemulsions produced by multidroplet flow-induced fusion. *Langmuir* **29**, 15787-15793 (2013).
24. Shum, H. C. *et al.* Droplet microfluidics for fabrication of non-spherical particles. *Macromol. Rapid. Communs.* **31**, 108-118 (2010).
25. Jeon, I. *et al.* Janus Graphene: Scalable Self-assembly and Solution-Phase Orthogonal Functionalization. *Adv. Mater.*, **31**, 1900438 (2019).
26. Amato, D. V., Lee, H., Werner, J. r. G., Weitz, D. A. & Patton, D. L. Functional Microcapsules via Thiol− Ene Photopolymerization in Droplet-Based Microfluidics. *ACS Appl. Mater. Interfaces* **9**, 3288-3293 (2017).
27. Nagelberg, S. *et al.* Reconfigurable and responsive droplet-based compound micro-lenses. *Nat. Commun.* **8**, 14673 (2017).
28. Zeininger, L. *et al.* Rapid Detection of Salmonella enterica via Directional Emission from Carbohydrate-Functionalized Dynamic Double Emulsions. *ACS Cent. Sci.* **5**, 789-795 (2019).
29. Goodling, A. E. *et al.* Colouration by total internal reflection and interference at microscale concave interfaces. *Nature* **566**, 523-527 (2019).
30. Zeininger, L. *et al.* Waveguide-based chemo-and biosensors: complex emulsions for the detection of caffeine and proteins. *Lab on a Chip* **19**, 1327-1331 (2019).
31. Lin, C.-J., Zeininger, L., Savagatrup, S. & Swager, T. M. Morphology-Dependent Luminescence in Complex Liquid Colloids. *J. Am. Chem. Soc.* **141**, 3802-3806 (2019).
32. Zarzar, L. D. *et al.* Dynamically reconfigurable complex emulsions via tunable interfacial tensions. *Nature* **518**, 520-524 (2015).
33. Li, T. *et al.* Particle-Stabilized Janus Emulsions that Exhibit pH-Tunable Stability. *Chem. Commun.* **55**, 5773-5776 (2019).
34. Kovach, I., Won, J., Friberg, S. E. & Koetz, J. Completely engulfed olive/silicone oil Janus emulsions with gelatin and chitosan. *Colloid Polym. Sci.* **294**, 705-713 (2016).
35. Concellón, A., Zentner, C. A. & Swager, T. M. Dynamic Complex Liquid Crystal Emulsions. *J. Am. Chem. Soc.* **141**, 18246-18255 (2019).
36. Atefi, E., Mann Jr, J. A. & Tavana, H. Ultralow interfacial tensions of aqueous two-phase systems measured using drop shape. *Langmuir* **30**, 9691-9699 (2014).
37. Zhou, C. *et al.* Microfluidic generation of aqueous two-phase-system (ATPS) droplets by oil-droplet choppers. *Lab on a Chip* **17**, 3310-3317 (2017).
38. Ge, L. L., Jin, H. M., Li, X., Wei, D. & Guo, R. Batch-Scale Preparation of Reverse Janus Emulsions. *Langmuir* **35**, 3490-3497 (2019).
39. Hann, S. D., Stebe, K. J. & Lee, D. AWE-somes: All Water Emulsion Bodies with Permeable Shells and Selective Compartments. *ACS Appl. Mater. Interfaces* **9**, 25023-25028 (2017).
40. Akamatsu, K., Kurita, R., Sato, D. & Nakao, S. Aqueous Two-Phase System Formation in Small Droplets by Shirasu Porous Glass Membrane Emulsification Followed by Water Extraction. *Langmuir* **35**, 9825-9830 (2019).
41. Cui, C., Zeng, C., Wang, C. & Zhang, L. Complex Emulsions by Extracting Water from Homogeneous Solutions Comprised of Aqueous Three-Phase Systems. *Langmuir* **33**, 12670-12680 (2017).
42. Song, Y. & Shum, H. C. Monodisperse w/w/w double emulsion induced by phase separation. *Langmuir* **28**, 12054-12059 (2012).
43. Guzowski, J., Korczyk, P. M., Jakiela, S. & Garstecki, P. The structure and stability of multiple micro-droplets. *Soft Matter* **8**, 7269-7278 (2012).

Acknowledgements

The authors gratefully acknowledge funding by the Max-Planck society. M.P. acknowledges financial support from the Swiss National Science Foundation with the project number P2GEP2_181528.; B.S. acknowledges the University of Glasgow for financial support;; L.Z. is grateful for financial support through the Emmy-Noether program of the German Research Foundation (DFG) (grant no: ZE1121-3). We also thank Dr. Clemens Liedel (MPI-KG) for kindly providing access to the ITC.

Competing interests

The authors declare no competing interests.

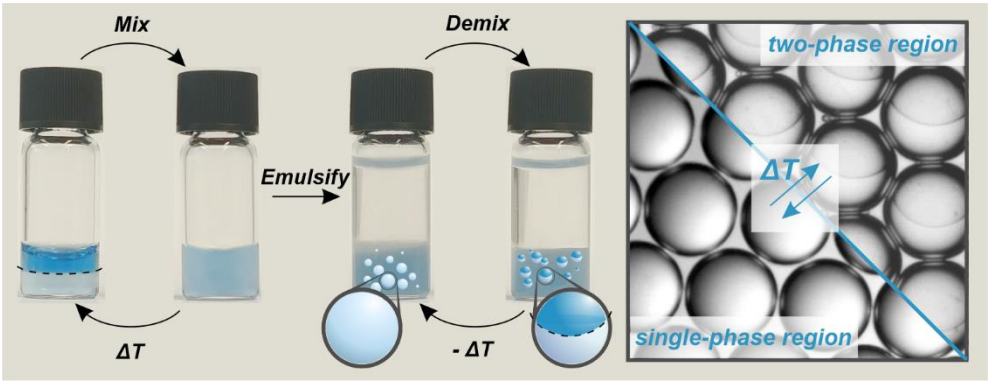
Mix
Demix
Emulsify
ΔT
- ΔT
two-phase region
ΔT
single-phase region

CRediT author statement:

Marko Pavlovic: Data curation, Methodology, Investigation, Writing - original draft; Markus Antonietti: Conceptualization, Writing - review & editing; Bernhard Schmidt: Conceptualization, Writing - review & editing; Lukas Zeininger: Conceptualization, Investigation, Supervision, Writing - original draft, Writing - review & editing